第 26 回日本バーチャルリアリティ学会大会論文集（2021 年 9 月）

Superimposing Methane Gas Visualization over a Real Environment Using Optical See-through Augmented Reality

Liyuan DUAN[1), 松倉悠 [2), プンポンサノン・パリンヤ [1), 岩井大輔 [1), 佐藤宏介 [1)
Liyuan DUAN, Haruka MATSUKURA, Parinya PUNPONGSANON, Daisuke IWAI, and Kosuke SATO

1) 大阪大学 基礎工学研究科 （〒 560-8531 大阪府豊中市待兼山町 1-3, liyuan@sens.sys.es.osaka-u.ac.jp, {parinya, daisuke.iwai, sato}@sys.es.osaka-u.ac.jp）
2) 電気通信大学 情報理工学研究科 （〒 182-8585 東京都調布市調布ヶ丘 1-5-1, matsukura@uec.ac.jp）

概要: At landfill sites, monitoring methane gas is the major method to supervise and validate landfill sites stabilization and safety. The results that previous methods generate by sophisticated sensors and show on a monitor display can confuse workers due to the mismatching between digital and actual gas positions. Therefore, we introduce Augmented Reality (AR) technology that can display the gas visualization over the real environment directly to check the gas position more easily. In this paper, the calibration method superimposes the virtual image onto a real experimental field and preliminary experimental results are reported.

キーワード： Optical see-through HMD, AR, visualization, methane gas

1. Introduction

While most gases are invisible by human eyes, people in technical fields need to observe the gas characteristics to predict its behavior. In a specific scenario, visualization of gas is required, such as in landfill sites and chemical plants. In this research, we will use landfill gas as an example to detect.

Landfill gas is produced during decomposition after the organic waste is buried in the municipal waste landfill. The component of landfill gas is approximately 50 percent of methane (CH_4), and 50 percent composed of carbon dioxide (CO_2), hydrogen sulfide (H_2S), etc. [5]. All these gases are harmful to human health and the environment. For example, hydrogen sulfide can pollute groundwater, soil near the landfill site. Among all these landfill gases, methane gas has been continuously focused on because of its flammability and global warming potential, making methane the major factor of greenhouse gas. The ability to catch and keep heat in the atmosphere of methane is 21 times greater than carbon dioxide. Monitoring methane is the main way to supervise stabilization of landfill sites and confirm the safety of landfill sites and surrounding areas.

Traditionally, the chamber method is applied to monitor methane's concentration value by placing it at a specific gas emission point [6]. To apply the chamber method more efficiently, engineers develop several gas distribution mapping algorithms to find out the emission point [4]. However, the mismatching between digital graphs and the real environment can confuse workers where the actual position is. A method that uses an infrared filter visualizes gas directly by using a camera [3] remotely. Virtual reality (VR) technology is another way to image gas models with simulated environments using Head-Mounted Display (HMD). However, wearing a VR headset only shows graphics information and leaves the user blind to the real world, making Augmented Reality (AR) come. As the combination of the efforts from previous research, AR technology aims to explore the visualization technique for gas detection for the efficiency of finding gas sources with people and robots.

2. System Overview

2.1 Measuring Device and Display Device

The system we developed is shown in Fig.1. We used a laser gas detector, motion capture cameras, and an AR Head-Mounted Display (HMD) to visualize detected gas information (e.g., gas concentration and position) in near real-time. The user wears the AR HMD (Microsoft HoloLens 2^{nd} generation) and holds the laser methane detector (Laser Methane mini SA3C32B-BJ, Tokyo Gas Engineering Solution), hereinafter referred to as LMm,

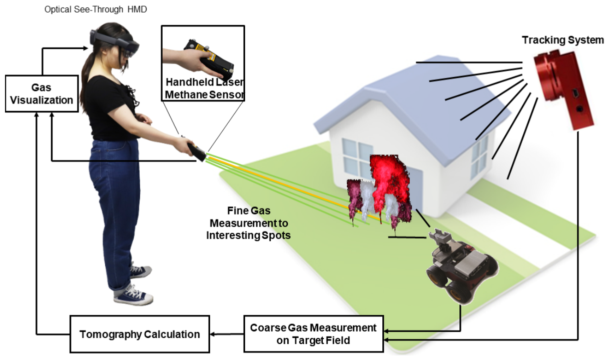

図 1: Our proposed gas visualization system: a user wears the AR glasses while using a gas detector. Detected gas information is converted into graphics visualization displayed through the AR glasses.

moves within the cover range of infrared motion capture cameras (OptiTrack Flex3, NaturalPoint Inc), hereinafter referred to as Flex3. The system collects gas information from LMm, and location data from Flex3, where the user points to LMm. Then, after the calculation of gas parameters and conversion to visualization parameters, the final gas distribution is displayed on the AR HMD. When the user is not online, the robot can act as offline detection to continuously monitor and supervise the field's safety.

2.2 Tracking System

In the motion capture part, Flex3 can capture any light whose wavelength is longer than 800 nm by applying an IR pass filter. Inside Flex3 software, the target object can be captured by a 3D model built by a captured light spot. Therefore, we use sphere markers with 3M 7610 Reflective Tape, which can reflect acceptable light, be captured at any angle, adhesive them on LMm, and let Flex3 provide LMm's position and rotation data. Depending on these motion data, the gas's position where LMm is pointing and detecting can be calculated successfully.

2.3 Gas Measurement and Mapping Visualization

The measured value obtained from LMm is expressed by the methane column density, which means LMm integrates all detected gas concentration values on the whole laser path. In other words, it isn't easy to independently get the value of the gas concentration of points directly from LMm. Therefore, we grind our target detection field to 3D cells and map gas concentration into cells.

To visualize gas distribution, we use a couple of visual effects to show the characteristics of the gas, such as gas concentration, grid resolution, and position. Gas concentration refers to the density of methane detected by LMm; gas is the location where the gas is approximately.

The visualization model we developed has 3 types: ball, bar, and cloud to fit different scenarios, such as gas simulation inside detection process or data analysis after detection.

Color We use the RGB model to display gas concentration that R (red) changes from 0 to 255. For example, a redder model (R-value is closer to 255) displays a higher gas concentration and vice versa.

Size We use grid resolution as the bottom size of each visualization model, then other parts of size (e.g., height) change depending on gas concentration value. For example, the larger the gas concentration value is, the higher or bigger the visualization model represents. The height of bar and cloud, and radius of ball V_{size} is calculated based on the gas concentration G_{concs} and maximum gas concentration value G_{max} in the target detection field, and maximum size of visualization model V_{max} inside the target detection field. The formula we generate to calculate the size is shown as follow Equation 1:

$$V_{size} = \frac{G_{concs}}{G_{max}} \times V_{max} \quad (1)$$

Position The position of the cell in which LMm is pointed and the approximate location of detected gas.

2.4 System Workflow

The workflow of our system shows in Fig.2. There are 3 parts of our system's workflow: data input, data calculation, show models. The majority of our system is built by Unity which contains all calculations and model creation. Gas concentration values from LMm and motion data are sent to Unity through a WIFI connection. After the calculation and model's creation, the visualization is sent to AR HMD through a WIFI connection. Finally, the visualization appears inside the user's view.

2.4.1 Calibration

There are 2 separate coordinate systems in our system: Flex3 coordinate system and Unity coordinate system, which share the same coordination with the AR HMD system. The y axis of both Flex3 and Unity coordinate systems point up. For the accuracy of the final visualization model's position represented inside the user's view, calibrating these 2 independent coordinate systems are significant. We develop a procedure to calibrate these 2 systems. We make a calibrator that Flex3 can capture, and a virtual calibrator in Unity is the same as a physical calibrator, shown as Fig.3.

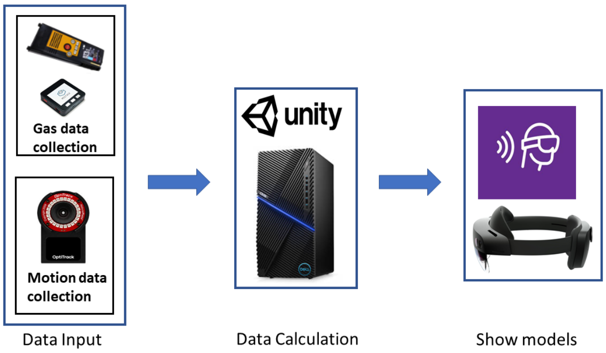

図 2: **Workflow of our system.**

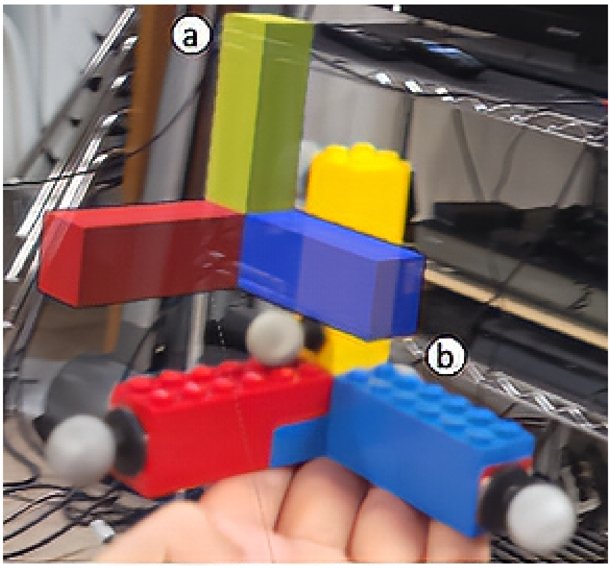

図 3: **The calibrators for system calibration: (a) virtual calibrator; (b) physical calibrator with markers.**

The user moves the physical calibrator until it is aligning with the virtual calibrator (they are completely superimposed), the system records the position of the physical calibrator's P_{pos}, the rotation degree of the physical calibrator on the y-axis P_{rot}, the position of the virtual calibrator V_{pos}, and the rotation degree of the virtual calibrator on y-axis V_{rot}, respectively. Then, the difference between P_{rot} and V_{rot} (D_{rot}), P_{pos} and V_{pos} (D_{pos}) is calculated. The calibration matrix is shown as the following Equation 2:

$$P_{Unity} = \begin{vmatrix} \cos(D_{rot}) & 0 & \sin(D_{rot}) & D_{pos_x} \\ 0 & 1 & 0 & D_{pos_y} \\ -\sin(D_{rot}) & 0 & \cos(D_{rot}) & D_{pos_Z} \\ 0 & 0 & 0 & 1 \end{vmatrix} \times P_{Flex3} \tag{2}$$

After calibration finishes, the user can start the detection procedure. The view of detection is shown in Fig.4.

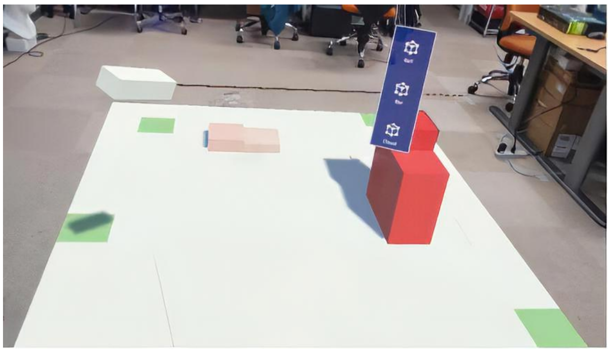

図 4: **A virtual green target field lays on the ground. Bars are created at the laser pointing position. The color and height represent gas concentration. The blue menu stays inside the right corner of the user view.**

A virtual green target field lays on the ground at the location of the physical target detection field. A white cube the same size as LMm with a red laser follows LMm's movement and notices the connection between the real and virtual world. While the user moves LMm, points inside the range of the target detection field, the model's size, color, and transparency belong to this pointed grid changes in near real-time depending on the received gas concentration value.

2.4.2 Mode Switching

There is a virtual menu inside the user's view (Fig.4) so that the user can always find it once the user wants to switch the visualization modes. When the user wants to switch the mode, use their finger to click the virtual menu or call the wanted mode's name; the mode is switched and continues the detection.

3. Experiment

3.1 Experiment Field Setup

The experiment field setup diagram is designed as Fig.5, which is made in an indoor environment. The target detection field is set to a region of $2.0 \times 2.0[m]$. Around the target detection field, a $3.0 \times 3.0[m]$ region is set as user activity space. Both the user activity space and target detection field are covered by the detection of Flex3 from different directions. We set a grid for the target detection field by dividing it into 10 × 10 grid resolution with 0.2 [m] intervals.

During the whole process, the user is only allowed to move inside the user activity space. When in the detection process, to confirm the pointed cell receives accurate gas concentration, the user needs to stay at the same cell for 3 seconds. The total detection time of the whole target detection field is about 5 minutes.

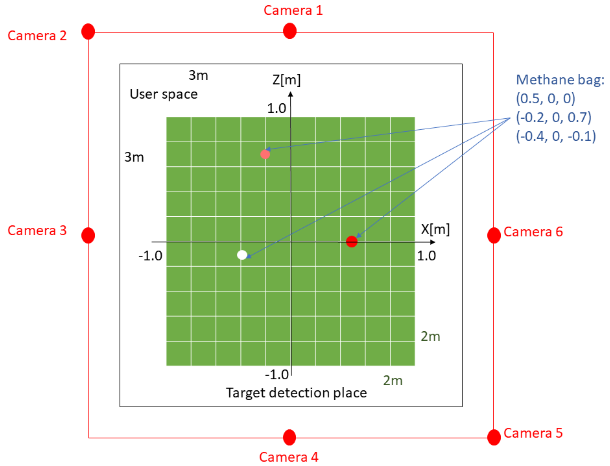

図 5: Schematic drawing of the experimental field.

There are 3 airbags ($0.2 \times 0.3m$) with different methane concentrations set in target detection field as shown in Fig.5, 30,000 ppm (3%) methane gas source (red point at right side of green target detection field in Fig.5) is arranged at (x, y, z) = (0.5, 0, 0), 10,000 ppm (1%) methane gas source (pink point at top left side of green target detection field in Fig.5) is arranged at (x, y, z) = (-0.2, 0, 0.7), and normal air level methane gas source (white point at center left side of green target detection field in Fig.5) is arranged at (x, y, z) = (-0.4, 0, -0.1).

3.2 Result

In Fig.6, we compare physical methane bags position and virtual gas distribution visualization represented by the bar mode. By applying Eq.2, the virtual target field is closely fit into the physical target detection field. As mentioned before, the redder model represents higher gas concentration, the color and height of models match the position of the methane bag: the 2 red high bars on the right side match with 30,000 ppm bag, the 2 pink middle-high bars at the top center side match with 10,000 ppm bag. The bar representing the airbag is blurred by similar air level bars, which are white and short. Because the length of the airbag (0.3 m) is longer than the cell (0.2 m), both pink and red are a group of 2 bars to visualize methane from 1 bag. The uneven density of methane causes the difference in height between 2 bars in 1 group, and the bag's position is not at the center point of the 2 cells.

4. Conclusions

This research discussed a new system that combines AR HMD, motion capture camera, and laser methane detector to visualize gas distribution in the real environment. We implemented an indoor environment experiment. The result showed that this system could successfully capture gas-existing areas on the floor and display the virtual bar visualization at the corresponding positions in the real world.

We will apply our system to a real gas leak situation in future work and investigate effective visualization modes for finding gas leaks quickly.

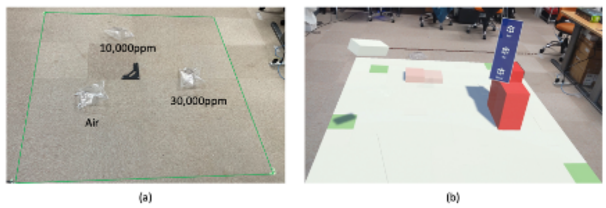

図 6: Final gas distribution visualization: (a) physical experiment field with 3 methane bags; (b) visualization result represented by bar mode.

Acknowledgement

JSPS KAKENHI Grant Number 19H02103 supported this work.

参考文献

[1] L. Duan, H. Matsukura, P. Punpongsanon, T. Hiraki, D. Iwai, and K. Sato: Adaptive Visualization of Gas Distribution Using Augmented Reality Glasses, 2020 IEEE 9th Global Conference on Consumer Electronics (GCCE), pp. 658–659, 2020.

[2] A. A. Al-Saffar and M. Al-Sarawi: Geo-visualization of the Distribution and Properties of Landfill Gases at Al-Qurain Landfill, Kuwait, Kuwait Journal of Science, Vol. 45, No. 3, pp. 93–104, 2018.

[3] J. Sandsten, H. Edner, and S. Svanberg: Gas Visualization of Industrial Hydrocarbon Emissions, Optics Express, Vol. 12, No. 7, pp. 1443-1451, 2004.

[4] M. Inagaki, H. Matsukura, D. Iwai and K. Sato: Application of Compressed Sensing to Measurement of Methane Gas Distribution, Proceedings of SICE 2019, pp. 1553–1556, 2019.

[5] National Research Council, Emergency and Continuous Exposure Limits for Selected Airborne Contaminants: Volume 1, The National Academies Press, Washington, DC, 1984. Available from: https://www.nap.edu/catalog/689/emergency-and-continuous-exposure-limits-for-selected-airborne-contaminants-volume

[6] J. Bogner, M. Vogt, and R. Piorkowski: Landfill Gas Generation and Migration: Review of Current Research II, 1989. Available from: https://www.osti.gov/servlets/purl/6347445

